

Synthesis and structural studies of cation-substituted Aurivillius phases $ASrBi_2Nb_2TiO_{12}$

Qingdi Zhou^a, Brendan J. Kennedy^{a,*}, Margaret M. Elcombe^b

^a*School of Chemistry, The University of Sydney, Sydney, NSW 2006, Australia*

^b*Bragg Institute, ANSTO, Menai, NSW 2234, Australia*

Received 8 June 2006; received in revised form 10 August 2006; accepted 11 August 2006

Available online 15 August 2006

Abstract

We report here a novel method to prepare high-quality samples of the three layered oxides $ASrBi_2Nb_2TiO_{12}$ $A = Ca, Sr$ or Ba using the pre-formed intermediates $ABi_2Nb_2O_9$ and $SrTiO_3$. The room temperature structures were refined using synchrotron X-ray and Neutron powder diffraction data in the orthorhombic space group $B2cb$. This symmetry arises as a consequence of cooperative tilting of the BO_6 octahedra in the $[ASrNb_2TiO_{10}]^{2-}$ perovskite-like slabs and a polar displacement of the cations. The structure is characterized by extensive cation disorder but lacks appreciable oxygen vacancies.

© 2006 Elsevier Inc. All rights reserved.

Keywords: Aurivillius oxide; Ferroelectric oxide; Cation disorder

1. Introduction

The bismuth layered perovskites of the type $[Bi_2O_2][A_{n-1}B_nO_{3n+1}]$ are generally described as Aurivillius phases in recognition of the pioneering work of B. Aurivillius over 50 years ago [1]. These oxides have a common structural motif consisting of ABO_3 perovskite-like groups separated by $[Bi_2O_2]^{2+}$ layers. The majority of these oxides are ferroelectric at room temperature as a consequence of the displacement of the B -type cations from the center of the BO_6 octahedra [2,3]. The Bi^{3+} cations in the $[Bi_2O_2]^{2+}$ layers have a stereochemically active $6s^2$ lone pair of electrons that extends towards the perovskite A -site repelling the surrounding oxygen anions. Atomic displacements along the a axis from the corresponding positions in the parent tetragonal ($I4/mmm$) structure cause ferroelectric spontaneous polarization [4]. To date, a large number of cations have been incorporated into the A -site, most commonly Bi^{3+} , Ln^{3+} , Pb^{2+} , Ca^{2+} , Sr^{2+} , Ba^{2+} , Na^+ , K^+ , etc. Much fewer cations occupy the perovskite B -site cations, most importantly Ti^{4+} , Nb^{5+} , Ta^{5+} , W^{6+}

and Mo^{6+} , with substitution by Ga^{3+} and Al^{3+} well documented [5–7]. The inability to substitute other cations on the B -site limits the ability of these oxides to be tuned for particular applications, and contrasts with the remarkable compositional flexibility of B -type cations found in ABO_3 perovskites [7].

A challenge of modern solid-state chemistry is to develop synthetic methods to prepare oxides with structures and compositions that are not accessible using conventional “shake-and-bake” methods. In the case of layered perovskite oxides, the pioneering work of Whittingham and Jacobson [8] has demonstrated that the properties of such oxides can be tuned by intercalating suitable ions or small molecular species. The topotactic addition of such species provides a mechanism to develop still more complex structures. Recently, Sivakumar and Gopalakrishnan [9] have shown it is possible to form Aurivillius-type oxides from layered Ruddlesden–Popper or Dion–Jacobson type oxides by metathesis reactions with $PbBiO_2Cl$. The same group also recently reported that reaction of $n = 2$ Aurivillius oxide $SrBi_2Nb_2O_9$ with the perovskite $NaTaO_3$ yielded the $n = 3$ oxide $SrNaBi_2Nb_2TaO_{12}$ under mild conditions [10]. These studies demonstrate that it is possible to build-up complex inorganic structures from

*Corresponding author. Fax: +61 29351 3329.

E-mail address: kennedyb@chem.usyd.edu.au (B.J. Kennedy).

simpler building blocks, in a manner analogous to that routinely used in molecular systems.

The aim of the present work was to prepare some mixed metal Nb–Ti Aurivillius oxides using preformed oxides and to determine the precise structures of these oxides. In contrast to previous work [11], we show these materials have orthorhombic symmetry and do not show appreciable oxygen vacancies. A longer-term ambition of this work is to incorporate paramagnetic transition metals ions into such structures [12].

2. Experimental

All starting materials, including SrTiO₃, were obtained from Aldrich Chemicals and used without purification. Crystalline samples of $ABi_2Nb_2O_9$ ($A = \text{Ca, Sr, Bi}$) were synthesized using conventional solid-state methods from stoichiometric amounts of Bi₂O₃, Nb₂O₅ and ACO₃ [13]. These were mixed and heated at 700 °C/12 h, 800 °C/24 h, 900 °C/24 h and 1000 °C/60 h, with intermediate regrinding.

To prepare the $ASrBi_2Nb_2TiO_{12}$ samples, appropriate amounts of $ABi_2Nb_2O_9$ and SrTiO₃ were weighed, mixed in the presence of acetone, and heated at 1000 °C/72 h for $A = \text{Ca}$ and, 1000 °C/180 h and 1050 °C/36 h for $A = \text{Sr}$ and Ba, and with periodic regrinding. The bulk compositions of the samples were confirmed using X-ray fluorescence spectroscopy and the homogeneity of the samples verified using high-resolution scanning electron microscopy. Back-scattering SEM images showed no evidence for any segregation.

The reactions were followed by powder X-ray diffraction using CuK α radiation on a Shimadzu D6000 diffractometer. Synchrotron X-ray diffraction data were recorded on the Debye Scherrer diffractometer at the Australian National Beamline Facility, Beamline 20B at the Photon Factory [14]. The samples were housed in 0.3-mm diameter capillaries that were rotated during the measurements. Data were collected in the angular range $5 < 2\theta < 85^\circ$, step size 0.01° using X-rays of wavelength 0.8028 Å.

Neutron powder diffraction data were collected at room temperature with the high-resolution powder diffractometer at the Australian Research Reactor, HIFAR ($\lambda = 1.885$ Å, $10 < 2\theta < 150^\circ$, step size 0.05°) [15]. The samples were housed in vanadium containers throughout the measurements.

Refinements of the crystal structures were performed with program RIETICA [16]. The diffraction peaks were described by a pseudo-Voigt function where a Lorentzian contribution to the Gaussian peak shape is refined. For the neutron diffraction studies, a correction for peak asymmetry was made. The background was described by a six-parameter polynomial. For the X-ray profiles, the background was estimated by interpolation between up to 40 user-selected points. The 00*l*-type reflections in the synchrotron data were systematically broader than nearby reflections and an anisotropic peak-broadening parameter was included in the refinements.

3. Results and discussion

3.1. Space group and symmetry

Powder X-ray diffraction patterns showed that the direct reaction of $ABi_2Nb_2O_9$ and SrTiO₃ yielded pure samples of the $n = 3$ Aurivillius oxides $ASrBi_2Nb_2TiO_{12}$. These oxides have previously been prepared by using direct reaction of the five constitute cations at 1100 °C [11]. The powder X-ray diffraction patterns, recorded using CuK α radiation, could be indexed using the tetragonal ($I4/mmm$) cells reported by Haluska and Misture [11]. The related three-layered oxide Bi₄Ti₃O₁₂ is a well-known ferroelectric that crystallizes in the non-centrosymmetric $B2cb$ space group, whose structure is characterized by both tilting of the TiO₆ octahedra and polar displacements of the cations [17–19]. Synchrotron diffraction patterns were collected for the three oxides and, as is evident from Fig. 1, there is no evidence of any peak splitting indicative of lower symmetry. In particular, the 137 reflection $2\theta = 28^\circ$ is a singlet in all three patterns, this being allowed to split in orthorhombic, $B2cb$, symmetry. This is somewhat surprising, since the symmetry of the perovskites is very sensitive to geometric considerations, as exemplified by the Goldschmidt tolerance factor. By analogy with the $n = 2$ oxides, $ABi_2Nb_2O_9$, $A = \text{Ca, Sr, Ba}$, it is expected that reduction in the size of the A -site cation will lead to less than optimal A –O bonding interactions, unless co-operative tilting of the BO_6 octahedra occurs [13,20]. Such tilting lowers the symmetry from tetragonal to, in the case of the $n = 3$ oxides, orthorhombic. The smaller the cation the larger the magnitude of tilting and subsequently the orthorhombic distortion.

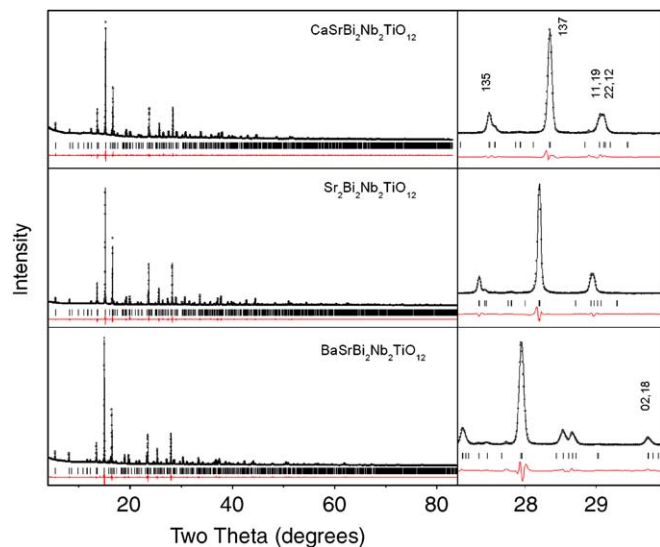


Fig. 1. Observed, calculated and difference synchrotron X-ray diffraction data for $ASrBi_2Nb_2TiO_{12}$. The tick marks show the positions allowed for the orthorhombic space group $B2cb$. The panels on the RHS highlight the small size of the orthorhombic distortion.

Since the tilting is associated with cooperative displacement of the oxygen anions, we sought evidence for this using powder neutron diffraction. The neutron diffraction patterns for $\text{CaSrBi}_2\text{Nb}_2\text{TiO}_{12}$ shows an obvious, but weak, 121/211 reflections near $2\theta = 45^\circ$ indicative of such tilting. The intensity in this region is observed to decrease as the size of the *A*-type cation increases, and in $\text{BaSrBi}_2\text{Nb}_2\text{TiO}_{12}$ there is little if any obvious intensity in this region of the diffraction pattern. The synchrotron patterns do not show a similar systematic decrease in intensity for the same reflections (observed near $2\theta = 18.8^\circ$ at $\lambda = 0.8028 \text{ \AA}$, demonstrating these are associated with the oxygen anions, rather than the cations. It was not possible to index these reflections without an increase in the cell parameters, nor was it possible to fit this region of the neutron diffraction profiles in $I4mm$, an alternative tetragonal space group observed in $\text{BaBi}_2\text{Nb}_2\text{O}_9$ [21].

While these additional 121/211 reflections overlap with the 01,12 and 026/206 reflections in the neutron diffraction patterns, the Rietveld analysis shows these latter three reflections contribute little, neutron, intensity in this region. The Rietveld analysis suggests the intensity of the 01, 12 and 026/206 neutron reflections does not significantly change through the series. The 026/206 reflection is the strongest reflection in this portion of the X-ray patterns and the relative intensity of this increases as the size of the *A*-type cation increases. It is possible that $\text{BaSrBi}_2\text{Nb}_2\text{TiO}_{12}$ may be tetragonal, as reported by Haluska and Misture [11], although we find the neutron diffraction profile for the $\text{BaSrBi}_2\text{Nb}_2\text{TiO}_{12}$ to be better fitted in $B2cb$ (R_p 2.68% R_{wp} 3.35%) than in $I4/mmm$ (R_p 3.24%, R_{wp} 4.48%) with 0.03% orthorhombic distortion $a = 5.5477(7)$ $b = 5.5463(7)$ \AA . The intensity of the superlattice reflections shows that the Ca and Sr oxides clearly have the lower symmetry, although we note that all three oxides are, within the resolution of our diffractometers, metrically tetragonal. Such pseudo-symmetry is relatively common in oxides with perovskite-type structures [22].

Subsequently, we refined the structure using the synchrotron X-ray and neutron diffraction data in the orthorhombic space group $B2cb$ (Fig. 2), and the final Rietveld profiles are shown in Figs. 1 and 2. Fig. 3 compares the fits in $I4/mmm$ and $B2cb$ for $\text{CaSrBi}_2\text{Nb}_2\text{TiO}_{12}$. A representation of the structure is shown in Fig. 4. This space group not only allows for tilting of the octahedra but also for a polar displacement of the cations along the *a*-axis. The refined structural parameters are listed in Tables 1–3 and selected bond distances in Table 4. In the structural refinements, the positions of the two types of cations (*A* or Bi) in the $[\text{Bi}_2\text{O}_2]^{2+}$ layers have been treated as independent to reflect the stereochemical influence of the Bi 6*s* lone pair electrons. The observed pseudo-symmetry of the structures coupled with the use of long-wavelength neutrons results in higher than typical esds for the atomic coordinates, there being no obvious correlations in the refinements that could account for the magnitude of the esds.

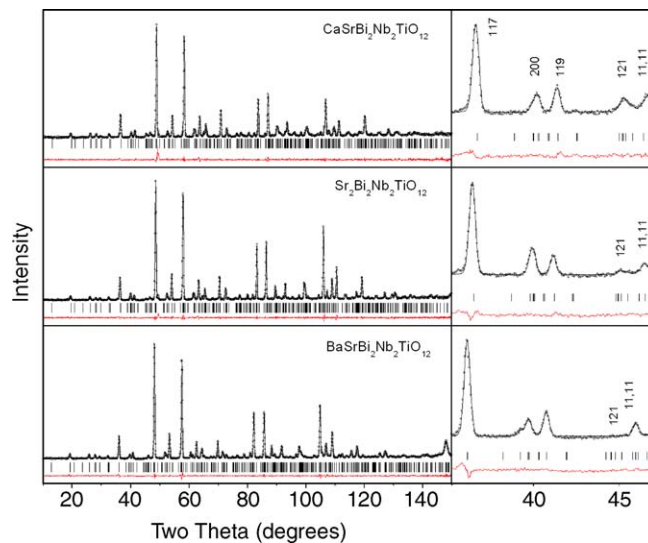


Fig. 2. Observed, calculated and difference neutron diffraction data for $\text{ASrBi}_2\text{Nb}_2\text{TiO}_{12}$. The tick marks show the positions allowed for the orthorhombic space group $B2cb$. The panels on the RHS illustrate the changing intensity of the reflections associated with the tilting of the octahedra.

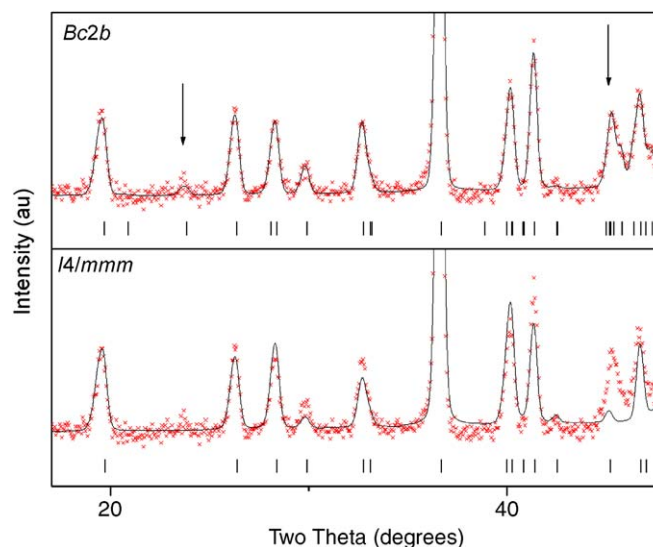


Fig. 3. Portions of the neutron diffraction profiles for $\text{CaSrBi}_2\text{Nb}_2\text{TiO}_{12}$ fitted in both $I4/mmm$ and $B2cb$ illustrating the superior fit of the latter. Note in particular the region around $2\theta = 45^\circ$ due to the 121 reflection. There is also evidence of some intensity near $2\theta = 23.4^\circ$ indicative of a 014 reflection that is systematically forbidden in the tetragonal space group.

Mandal et al. [10] recently postulated that the incorporation of cations, such as Sr, that lack a s^2 lone pair electron into the perovskite slabs may force the structure to remain centrosymmetric. The demonstration here that the oxides $\text{ASrBi}_2\text{Nb}_2\text{TiO}_{12}$ where the perovskite-type *A* site contains appreciable amounts of alkaline earth cations and have structures that can be refined in the non-centrosymmetric space group $B2cb$ demonstrates this postulate to be

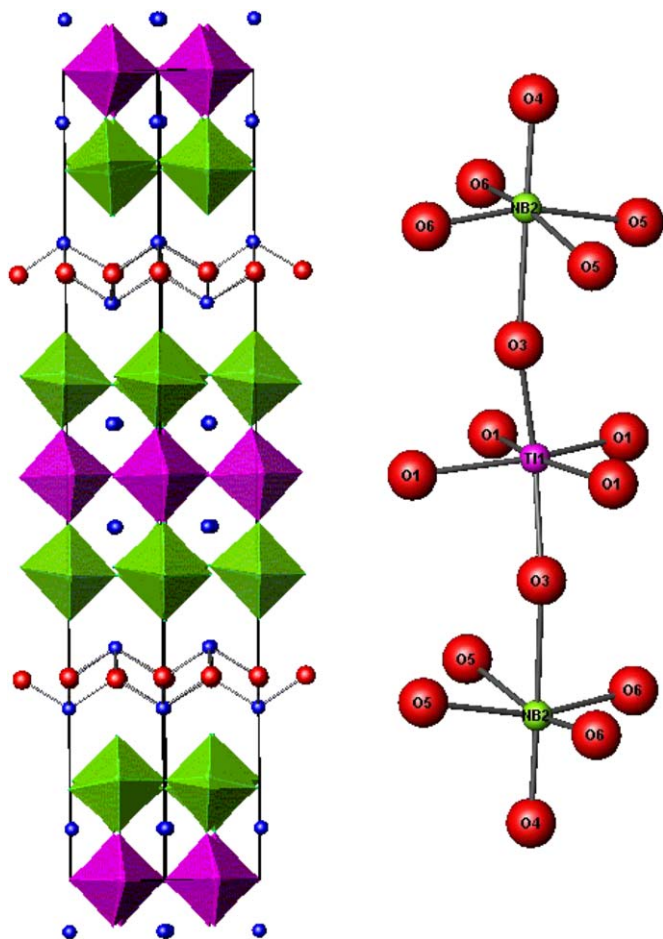


Fig. 4. (a) Representation of the crystal structure of the $n = 2$ Aurivillius phase $\text{CaSrBi}_2\text{Nb}_2\text{TiO}_{12}$ in space group $B2cb$. (b) details of the coordination environment of the Nb and Ti atoms.

incorrect. Indeed the well-known ferroelectric oxides $A\text{Bi}_2\text{B}_2\text{O}_9$, $B = \text{Nb, Ta}$ also have a non-centrosymmetric structure and contain an extensive amount of the A -type cation in the perovskite-type slabs [13,23]. These oxides have the common feature of containing small d^0 cations that are susceptible to a second-order Jahn–Teller distortion. Since oxides such as $\text{Bi}_2\text{Sr}_2\text{Nb}_{2.5}\text{Fe}_{0.5}\text{O}_{12}$ are centrosymmetric [10]; it is more likely that the loss of centrosymmetry is related to the incorporation of the larger d^5 Fe^{3+} cation into the perovskite layers, and it may be this feature that limits the range of cations that can exist on the B -site.

3.2. Cation disorder

An important structural feature of these oxides is the extent and nature of the cation disorder. It is now well established that a small amount of disorder between the Bi cations in the $[\text{Bi}_2\text{O}_2]^{2+}$ layers and the A -type cations in the $[\text{A}_{n-1}\text{B}_n\text{O}_{3n+1}]^{2-}$ perovskite slabs occurs [12,24–27]. In the present case, disorder between Nb and Ti, the two perovskite B -type cations, over the inner and outer sites is also possible. In estimating the site occupancies, the following assumptions were made: (a) all cation sites were fully occupied; (b) the ADPs of cations on the same sites were identical; (c) the positions of all cations in the $M(1)$ site were identical; however, the Bi on the $M(2)$ site could occupy a different position from the alkaline earth cations. These assumptions are similar to that used by other workers [14]. The isotropic displacement parameter for the $M(1)$ site is expected to be larger than that of the $M(2)$ site due to more distorted geometry of this site. This is observed in the refinements for the Ca and Sr oxides. In the Ba-containing oxide, the displacement parameter for

Table 1
Final atomic coordinates and isotropic atomic displacement parameters for $\text{CaSrBi}_2\text{Nb}_2\text{TiO}_{12}$ at room temperature

Atom	x	y	z	Biso (\AA^2)	N
Ca(1)	0	1.021(2)	0.0641(2)	2.2(2)	0.32(1)
Bi(1)	0	1.021(2)	0.0641(2)	2.2(2)	0.18(1)
Sr(1)	0	1.021(2)	0.0641(2)	2.2(2)	0.50(1)
Ca(2)	0.990(12)	0.942(10)	0.2218(11)	1.2(2)	0.18(1)
Bi(2)	1.015(3)	1.016(1)	0.2121(2)	1.2(2)	0.82(1)
Sr(2)	0.990(12)	0.942(10)	0.2218(11)	1.2(2)	0.00(1)
Nb(1)	0.025(4)	0	0.5	0.7(3)	0.282(3)
Ti(1)	0.025(4)	0	0.5	0.7(3)	0.218(3)
Nb(2)	0.013(4)	1.019(2)	0.3739(2)	0.1(2)	0.718(3)
Ti(2)	0.013(4)	1.019(2)	0.3739(2)	0.1(2)	0.282(3)
O(1)	0.717(3)	0.305(2)	−0.0003(4)	2.5(2)	1
O(2)	0.257(3)	0.247(8)	0.2480(3)	0.8(1)	1
O(3)	0.016(3)	1.042(2)	0.4418(2)	1.5(2)	1
O(4)	1.011(4)	1.022(2)	0.3195(2)	3.6(2)	1
O(5)	0.280(3)	0.245(4)	0.1223(3)	2.6(2)	1
O(6)	0.243(3)	0.249(3)	0.8861(2)	0.6(2)	1

$a = 5.4745(5)$, $b = 5.4746(5)$ and $c = 33.0661(9)$ \AA . Full occupancy of the $4a$ Nb(1) site is $N = 0.5$. All atoms are in general position $8b$ except, Nb(1) that is on the $4a$ site.

Table 2
Final atomic coordinates and isotropic atomic displacement parameters for Sr₂Bi₂Nb₂TiO₁₂ at room temperature

Atom	<i>x</i>	<i>y</i>	<i>z</i>	Biso (Å ²)	<i>N</i>
Sr(1)	0	1.005(2)	0.0634(1)	1.87(8)	0.81(1)
Bi(1)	0	1.005(2)	0.0634(1)	1.87(8)	0.19(1)
Sr(2)	1.005(2)	0.002(2)	0.1987(6)	1.30(8)	0.19(1)
Bi(2)	1.005(2)	0.002(2)	0.2144(1)	1.30(8)	0.81(1)
Nb(1)	0.020(8)	0	0.5	1.1(4)	0.255(3)
Ti(1)	0.020(8)	0	0.5	1.1(4)	0.245(3)
Nb(2)	0.002(3)	1.024(3)	0.3728(1)	0.2(1)	0.745(3)
Ti(2)	0.002(3)	1.024(3)	0.3728(1)	0.2(1)	0.255(3)
O(1)	0.714(3)	0.287(2)	0.0003(4)	1.4(1)	1
O(2)	0.248(2)	0.248(7)	0.2509(4)	1.0(1)	1
O(3)	0.004(3)	1.011(3)	0.4414(1)	1.3(1)	1
O(4)	1.000(3)	1.013(3)	0.3184(1)	2.1(1)	1
O(5)	0.259(2)	0.256(3)	0.1156(2)	0.7(2)	1
O(6)	0.233(2)	0.244(3)	0.8789(2)	1.1(2)	1

$a = 5.5051(5)$, $b = 5.5057(6)$ and $c = 33.1947(14)$ Å.

Table 3
Final atomic coordinates and isotropic atomic displacement parameters for BaSrBi₂Nb₂TiO₁₂ at room temperature

Atom	<i>x</i>	<i>y</i>	<i>z</i>	Biso (Å ²)	<i>N</i>
Ba(1)	0	0.998(2)	0.0638(1)	2.24(7)	0.27(1)
Bi(1)	0	0.998(2)	0.0638(1)	2.24(7)	0.25(1)
Sr(1)	0	0.998(2)	0.0638(1)	2.24(7)	0.48(1)
Ba(2)	0.993(10)	−0.015(8)	0.1973(4)	0.75(8)	0.23(1)
Bi(2)	1.006(4)	0.013(2)	0.2158(1)	0.75(8)	0.75(1)
Sr(2)	0.993(10)	−0.015(8)	0.1973(4)	0.75(8)	0.02(1)
Nb(1)	0.020(8)	0	0.5	−0.03(3)	0.228(6)
Ti(1)	0.020(8)	0	0.5	−0.03(3)	0.272(6)
Nb(2)	−0.002(4)	0.990(3)	0.3728(1)	0.63(7)	0.772(6)
Ti(2)	−0.002(4)	0.990(3)	0.3728(1)	0.63(7)	0.228(6)
O(1)	0.726(3)	0.270(2)	−0.0003(3)	1.29(8)	1
O(2)	0.251(3)	0.253(3)	0.2469(2)	0.82(7)	1
O(3)	0.002(3)	1.008(2)	0.4415(1)	1.50(7)	1
O(4)	1.002(3)	0.994(2)	0.3193(1)	1.42(7)	1
O(5)	0.250(4)	0.257(3)	0.1181(2)	1.2(2)	1
O(6)	0.241(3)	0.244(2)	0.8815(2)	0.6(1)	1

$a = 5.5477(7)$, $b = 5.5463(7)$ and $c = 33.6566(5)$ Å.

Table 4
Selected bond lengths (Å) and bond valence sums for ASrBi₂Nb₂TiO₁₂

	Ca	Sr	Ba
Ti(1)–O(1) × 2	1.994(19)	2.034(14)	2.026(14)
Ti(1)–O(1) × 2	1.974(17)	1.921(13)	1.898(14)
Ti(1)–O(3) × 2	1.947(7)	1.948(3)	1.900(3)
Σ <i>v</i>	3.93	4.00	4.32
Nb(2)–O(3)	2.241(8)	2.278(5)	2.314(4)
Nb(2)–O(4)	1.794(8)	1.807(6)	1.801(4)
Nb(2)–O(5)	2.096(22)	2.079(20)	1.930(21)
Nb(2)–O(5)	1.936(23)	2.076(22)	1.965(21)
Nb(2)–O(6)	1.981(19)	1.922(18)	2.023(20)
Nb(2)–O(6)	1.831(20)	1.818(20)	2.017(20)
Σ <i>v</i>	5.39	5.23	4.99

the *M*(1) site is effectively zero, possibly reflecting absorption effects in this sample. Constraining the isotropic displacement parameters for the two sites to be

equal (that is $B_{\text{iso}} M(1) = B_{\text{iso}} M(2)$), did not alter either the refined occupancies or *R*-factors, but it did lead to an approximately three-fold increase in the uncertainty in the occupancies.

In the present work, we find that around 20% of the Bi atoms in the [Bi₂O₂]²⁺ layers are replaced by the *A*-type cation with the disordered Bi atoms occupying the perovskite *A*-sites. The extent of disorder is greatest in the Ba-containing oxide. The dependence of the disorder on the size of the *A*-type cation is similar that that seen in other systems and can be rationalized by bond valence sums [12]. In general, the *A*-site is underbonded and increasing the effective size of the cation on this site goes some way to mitigating this. Somewhat to our surprise, we observed a strong site preference in the two oxides with mixed *A*-type cations CaSr or BaSr. In both cases, the refinements suggested only Sr disorders onto the Bi₂O₂ layer with *A*-site exclusively occupied by Bi and Ca or Ba.

Haluska and Misture [11] observed a similar preference and reported that it was not possible to completely substitute Ca^{2+} or Ba^{2+} for Sr and concluded that $\text{BaSrBi}_2\text{Nb}_2\text{TiO}_{12}$ and $\text{CaSrBi}_2\text{Nb}_2\text{TiO}_{12}$ represented the solubility extremes for the series $A_x\text{Sr}_{2-x}\text{Bi}_2\text{Nb}_2\text{TiO}_{12}$.

The outer Nb(2) cation is displaced along the c -axis from the center of the NbO_6 octahedron towards the $[\text{Bi}_2\text{O}_2]^{2+}$ layer resulting in short Nb(2)–O(4) and long Nb(2)–O(3) bond distances. Due to the symmetry constraints the Ti(1) atom is not displaced along c but rather has two equal Ti–O(3) axial bonds. The refinements suggest that the cations occupying the Ti(1) and Nb(2) sites are also displaced along the a -axis with the inner Ti(1) atom exhibiting the greatest displacement. A similar trend was observed in $\text{Bi}_4\text{Ti}_3\text{O}_{12}$ where the Ti atoms occupying the inner site were displaced more than those on the outer site [18]. As noted above, such displacements contribute to the spontaneous polarization in these types of materials. In all three oxides, we observe a preference of the Ti for the inner Ti(1) site over the outer Nb(2) site. For a random distribution, n Nb(1) would be 0.333 and n Ti(1) = 0.167. The preference of Ti for the inner Nb1 site shows a small increase as the size of the A -cation increasing from 0.218 for $A = \text{Ca}$ to 0.272 for $A = \text{Ba}$.

3.3. Oxygen vacancies

In their recent study, Haluska and Misture [11] concluded that samples of $A\text{SrBi}_2\text{Nb}_2\text{TiO}_{12}$ were non-stoichiometric based on their structural refinements in $I4/mmm$ that revealed anomalously large ADP for O(1) and O(4). Constraining the ADP for these anions to a “reasonable” value allowed these authors to refine the oxygen occupancies, suggesting neither site was fully occupied. In the present work, the refinements in the orthorhombic $B2cb$ space group, showed the ADP’s for O(1) and O(4) have similar magnitudes to those of the other oxygen anions. We did, however, also observe anomalously large ADPs for these anions if the structures were refined in the, incorrect, tetragonal symmetry. For example B_{iso} for O(1) in $\text{CaSrBi}_2\text{Nb}_2\text{TiO}_{12}$ was $6.9(3) \text{ \AA}^2$ in $I4/mmm$ and 2.5 \AA^2 in $B2cb$. When the structure was refined in $B2cb$, not only were the ADPs more reasonable but the refined occupancy of the O(1) site was 1.03(2) and of the O(4) site 1.01(2), showing these sites to be fully occupied within the accuracy of the measurements. The observed behavior is consistent with the structure. The O(1) anion is in the equatorial plane of the TiO_6 octahedron and this anion moves significantly as the octahedra tilt. The O(4) anion connects the Bi and Nb cations. Large ADPs are typically observed for one of three reasons, vacancies in a particular site, the atom is located at an incorrect position in the refinement, typically placed on a higher symmetry general position or the atom shows static disorder away from a high symmetry site. For O(1), the behavior of the ADPs is indicative of orthorhombic, rather than tetragonal symmetry. For O(4), the higher than

usual ADP’s are thought to be due to static disorder of this anion as a consequence the disorder of the A -type cation into the Bi_2O_2 layers. We find no evidence, from the refinements for appreciable oxygen non-stoichiometry in these oxides.

4. Conclusion

We report here a novel method to prepare high-quality samples of the three-layered oxides $A\text{SrBi}_2\text{Nb}_2\text{TiO}_{12}$ $A = \text{Ca}, \text{Sr}$ or Ba using the pre-formed intermediates $A\text{Bi}_2\text{Nb}_2\text{O}_9$ and SrTiO_3 . The room temperature structures were refined using synchrotron X-ray and neutron powder diffraction data in the orthorhombic space group $B2cb$. This symmetry arises as a consequence of cooperative tilting of the BO_6 octahedra in the $[\text{ASrNb}_2\text{TiO}_{10}]^{2-}$ perovskite-like slabs and a polar displacement of the cations. The structure is characterized by extensive cation disorder but lacks appreciable oxygen vacancies. We speculate the differences between our work and that of Haluska and Misture [11] is not simply a consequence of the difference in the preparative method but rather reflects the superior resolution of our neutron diffraction data that affords better signal-to-noise statistics and has allowed the subtle lowering of symmetry to be detected.

Acknowledgments

This work has been partially supported by the Australian Research Council. The synchrotron diffraction measurements were supported by the Australian Synchrotron Research Program, which is funded by the Commonwealth of Australia under the Major National Research Facilities program. The Australian Institute of Nuclear Science and Engineering supported the neutron diffraction experiments. The assistance of Dr. James Hester with the synchrotron measurements is gratefully acknowledged.

References

- [1] B. Aurivillius, *Arkiv. Kemi.* 1 (1949) 463.
- [2] A.D. Rae, J.G. Thompson, R.L. Withers, *Acta Crystallogr., Sect. B* 48 (1992) 418.
- [3] E.C. Subbarao, *J. Phys. Chem. Solids* 23 (1962) 665.
- [4] Y. Shimakawa, Y. Kubo, Y. Tauchi, T. Kamiyama, H. Asano, F. Izumi, *Appl. Phys. Lett.* 77 (2000) 2749.
- [5] T. Rentschler, *Mater. Res. Bull.* 32 (1997) 351.
- [6] A. Castro, P. Millan, M.J. Martinez-Lope, J.B. Torrance, *Solid State Ion.* 63–65 (1993) 897.
- [7] R.H. Mitchell, *Perovskites: Modern and Ancient*, Almaz Press, Ont., Canada, 2002.
- [8] M.S. Whittingham, A.J. Jacobson (Eds.), *Intercalation Chemistry*, Academic Press, London, 1984.
- [9] T. Sivakumar, J. Gopalakrishnan, *Mater. Res. Bull.* 40 (2005) 39.
- [10] T.K. Mandal, T. Sivakumar, S. Augustine, J. Gopalakrishnan, *Mater. Sci. Eng. B* 121 (2005) 112.
- [11] M.S. Haluska, S.T. Misture, *J. Solid State Chem.* 177 (2004) 1965.
- [12] L. Viciu, J. Koenig, L. Spinu, W.L. Zhou, J.B. Wiley, *Chem. Mater.* 15 (2003) 1480.

- [13] Ismunandar, B.J. Kennedy, Gunawan, Marsongkohadi, J. Solid State Chem. 126 (1996) 135.
- [14] T.M. Sabine, B.J. Kennedy, R.F. Garrett, G.J. Foran, D.J. Cookson, J. Appl. Crystallogr. 28 (1995) 513.
- [15] C.J. Howard, C.J. Ball, R.L. Davis, M.M. Elcombe, Aust. J. Phys. 36 (1983) 507.
- [16] B.A. Hunter, C.J. Howard, Rietica for Windows, 1.7.7, Sydney, 1997.
- [17] A.D. Rae, J.G. Thompson, R.L. Withers, A.C. Willis, Acta Crystallogr., Sect. B 46 (1990) 474.
- [18] C.H. Hervoches, P. Lightfoot, Chem. Mater. 11 (1999) 3359.
- [19] Q. Zhou, B.J. Kennedy, C.J. Howard, Chem. Mater. 15 (2003) 5025.
- [20] C.H. Hervoches, P. Lightfoot, J. Solid State Chem. 153 (2000) 66.
- [21] R.B. Macquart, B.J. Kennedy, T. Vogt, C.J. Howard, Phys. Rev. B 66 (2002) 212102.
- [22] C.J. Howard, K.S. Knight, B.J. Kennedy, E.H. Kisi, J. Phys. C Condens. Matter 12 (2000) L677.
- [23] Y. Shimakawa, Y. Kubo, Y. Nakagawa, S. Goto, T. Kamiyama, H. Asano, F. Izumi, Phys. Rev. B 61 (2000) 6559.
- [24] R.B. Macquart, B.J. Kennedy, Y. Shimakawa, J. Solid State Chem. 160 (2001) 174.
- [25] S.M. Blake, M.J. Falconer, M. McCreedy, P. Lightfoot, J. Mater. Chem. 7 (1997) 1609.
- [26] Ismunandar, T. Kamiyama, A. Hoshikawa, Q. Zhou, B.J. Kennedy, Y. Kubota, K. Kato, J. Solid State Chem. 177 (2004) 4188.
- [27] Ismunandar, B.J. Kennedy, Hunter, Solid State Ion. 112 (1998) 281.